Available online at www.sciencedirect.com
ScienceDirect
European Journal of Medicinal Chemistry 43 (2008) 2262–2267
EUROPEAN JOURNAL OF MEDICINAL CHEMISTRY
http://www.elsevier.com/locate/ejmech

Short communication

Synthesis, molecular modeling studies and selective inhibitory activity against MAO of *N*1-propanoyl-3,5-diphenyl-4,5-dihydro-(1*H*)-pyrazole derivatives

Franco Chimenti [a], Rossella Fioravanti [a,*], Adriana Bolasco [a], Fedele Manna [a], Paola Chimenti [a], Daniela Secci [a], Francesca Rossi [a], Paola Turini [b], Francesco Ortuso [c], Stefano Alcaro [c], Maria Cristina Cardia [d]

[a] *Dipartimento di Studi di Chimica e Tecnologia delle Sostanze Biologicamente Attive, Università ''La Sapienza'', P.le Aldo Moro 5, 00185 Rome, Italy*
[b] *Dipartimento di Scienze Biochimiche ''A. Rossi Fanelli'' and Centro di Biologia Molecolare del CNR, Università di Roma ''La Sapienza'' P.le Aldo Moro, 5, 00185 Rome, Italy*
[c] *Dipartimento di Scienze Farmacobiologiche, Università di Catanzaro ''Magna Græcia'', Complesso Ninì Barbieri, 88021 Catanzaro, Italy*
[d] *Dipartimento Farmaco Chimico Tecnologico, Università degli Studi di Cagliari, Via Ospedale 72, 09124 Cagliari, Italy*

Received 18 October 2007; received in revised form 13 December 2007; accepted 14 December 2007
Available online 6 January 2008

Abstract

A series of *N*1-propanoyl-3,5-diphenyl-4,5-dihydro-(1*H*)-pyrazole derivatives were synthesized and assayed as inhibitors of MAO-A and MAO-B isoforms. Most of the tested compounds showed inhibitory activity with micromolar values and MAO-A selectivity. In addition a computational work was carried out on the most selective compound **3b** to highlight the most relevant interactions in the mechanism of recognition within both the MAO-A and the MAO-B enzyme active sites.

Keywords: Pyrazoline derivatives; MAO inhibitors; Molecular modeling

1. Introduction

The homeostasis of serotonin (5-HT), noradrenalin (NE) and dopamine (DA) in the brain is maintained by the removal of the amines from the synaptic cleft by a reuptake mechanism [1–3] and the oxidation by monoamine oxidase (MAOs) [4,5]. The flavin-containing mitochondrial enzyme monoamine oxidase MAO (EC 1.4.3.4.) is a key enzyme in regulating monoaminergic homeostasis and possibly neurotransmission. The action is achieved via the deamination in the central nervous system of neuroactive and vasoactive amines, such as dopamine, noradrenalin and serotonin.

Currently, two MAO isoforms encoded by separate genes sharing a common intron/exon organization [6–8] have been identified according to their substrate specificity: MAO-A, which preferentially metabolizes serotonin, and MAO-B, which has a greater affinity for phenylethylamine and benzylamine [9]. The two MAO isoforms can also be differentiated according to their inhibition by synthetic compounds: clorgyline and moclobemide for MAO-A and selegiline and lazabemide for MAO-B [10] (Fig. 1).

It has been suggested that MAO-A and MAO-B have distinctly different roles in monoamine metabolism.

One reason for this presumption is the fact that serotonergic neurons contain MAO-B, the isoenzyme that has a lower affinity for 5-HT. MAO-A preferentially oxidizes serotonin and noradrenalin, whereas MAO-B preferentially oxidizes phenylethylamine (PEA) [11,12]. Both forms can oxidize dopamine,

* Corresponding author. Tel.: +39 06 49913975; fax: +39 06 49913772.
E-mail address: rossella.fioravanti@uniroma1.it (R. Fioravanti).

0223-5234/$ - see front matter © 2008 Elsevier Masson SAS. All rights reserved.
doi:10.1016/j.ejmech.2007.12.026

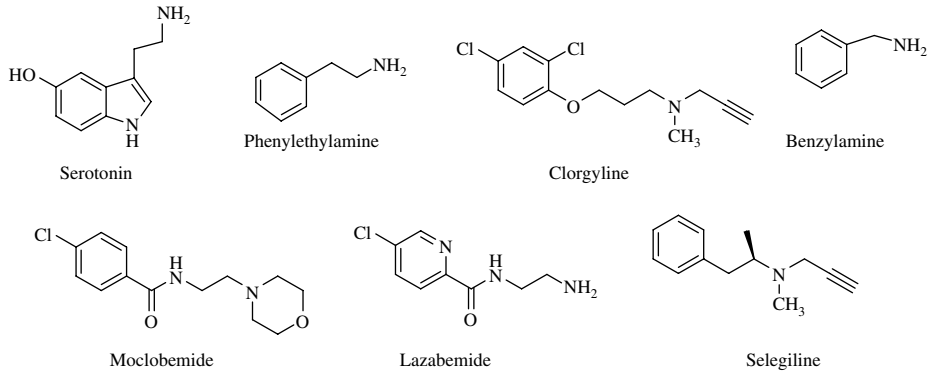

Fig. 1. Inhibitors and substrates of both MAO isoforms.

but MAO-A has a somewhat greater affinity for it in the rat brain. MAO-A exists predominantly in the catecholaminergic neurons and glia [13,14] whereas MAO-B is distributed in the serotonergic neurons, astrocytes, and glia [15].

The recent development of a new generation of highly selective, reversible MAO inhibitors has led to a renewed interest in the therapeutic potential of these compounds.

In particular, MAO-B inhibitors have been found to be useful as coadjuvants in the treatment of Parkinson's disease (PD) and Alzheimer's disease [16] (AD) where selective MAO-B inhibitors, such as selegiline, have been shown to protect neuronal cells from the consequences of oxidative stress in AD and PD patients [17]. The underlying mechanism of the effect of selegiline on the neuronal function is believed to be associated with decreased hydrogen peroxide (H_2O_2) production through MAO-B inhibition [18]. Previous studies have also stressed the role of impaired mitochondrial function and significant increases in monoamine oxidase (MAO) activities in the brains of both AD and PD patients, indicating that these enzymatic changes could contribute to oxidative stress through the formation of excessive H_2O_2. An excess of H_2O_2 is reported to cause lipid and protein peroxidation as well as the formation of toxic products, which have been shown to be involved in neuronal death in AD and PD [19]. Since multiple factors contribute to the pathology of AD, a recent approach in the treatment of this disease has been the development of drugs with multiple actions [20]. MAO-B inhibitors possessing diverse biochemical actions seem to be suitable candidates to solve this problem [21].

On the basis of this observation, we decided to design a strategy to synthesize novel MAO inhibitors (MAOIs). In previous communications [22–24] we have reported studies on the MAO inhibitory activity of different reversible MAO inhibitors, among which *N*1-acetyl, **1**, and *N*1-thiocarbamoyl pyrazolines, **2**, exhibited high potency along with good selectivity and due to their synthetic accessibility permitted a number of chemical changes. In order to better understand the role of the N1 substituent for inhibitory activity, in this communication we report on the synthesis of a new series of *N*1-propanoyl-3,5-diphenyl pyrazolines, **3**, with no changes in the A and B rings compared to the previous *N*1-acetyl and *N*1-thiocarbamoyl series (Fig. 2).

2. Chemistry

The synthesis of the *N*1-propanoyl-3,5-diphenyl pyrazolines, **3**, was performed according to the method shown in Scheme 1.

Treatment of the appropriate acetophenone with suitable benzaldehydes gave α,β-unsaturated ketones (chalcones) by a typical base-catalyzed aldol condensation in 50–80% yields, as shown in Scheme 1. Reaction of chalcones and hydrazine monohydrate in propionic acid afforded pyrazolines **3a–y**. The structures of **3a–y** were determined by their spectroscopic analysis. The chemical and physical data are reported in Table 1.

3. Biochemical assay

The inhibitory activities of compounds **3** were evaluated against both MAO-A and MAO-B isoforms as reported in Table 1.

All chemicals were commercial reagents of analytical grade, used without further purification. Bovine brain mitochondria were isolated according to Basford [25]. In all experiments the MAO activities of the beef brain mitochondria were determined by a fluorimetric method, according to Matsumoto et al. [26] using kynuramine as a substrate at four different final concentrations ranging from 5 μM to 0.1 mM. Briefly, the incubation mixtures contained: 0.1 mL of 0.25 M potassium phosphate buffer (pH 7.4), mitochondria (6 mg/mL), and drug solutions with final concentrations ranging from 0 to 10^{-3} μM. The solutions were incubated at 38 °C for 30 min. Addition of perchloric acid ended the reaction. The samples

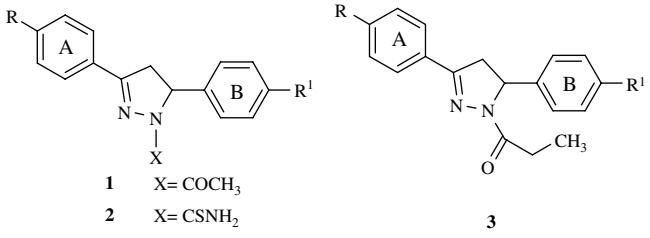

Fig. 2. General formula of derivatives **1**, **2** and **3**.

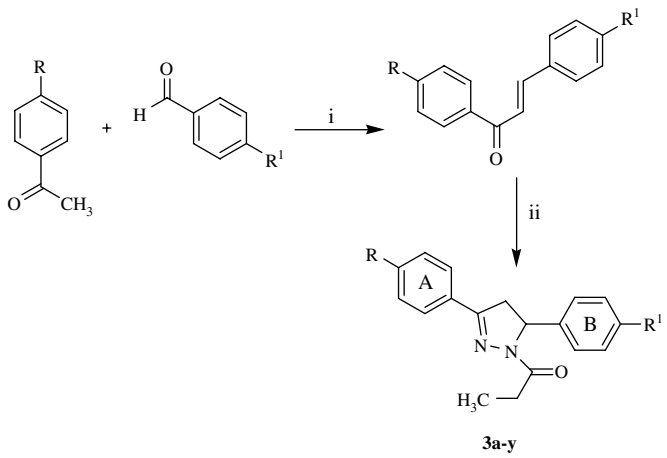

Scheme 1. Reagents and condition: (i) $Ba(OH)_2 \cdot 8H_2O$, EtOH, 25 °C; (ii) CH_3CH_2COOH, $NH_2NH_2 \cdot H_2O$, refluxed.

were centrifuged at 10,000g for 5 min, and the supernatant was added to 2.7 mL of 0.1 N NaOH. The pyrazole derivatives were dissolved in dimethyl sulfoxide (DMSO) and added to the reaction mixture in a concentration range from 0 to 10^{-3} mM. To study the inhibition of pyrazole derivatives on the activities of both MAO-A and MAO-B separately, the mitochondrial fractions were preincubated at 38 °C for 30 min before adding the specific inhibitors (L-deprenyl, 0.5 μM to estimate MAO-A activity, and clorgyline, 0.05 μM to assay the isoform B), considering that MAO-A is irreversibly inhibited by a low concentration of clorgyline, but is unaffected by a low concentration of L-deprenyl, which is used in the MAO-B form. Fluorimetric measurements were recorded with a Perkin-Elmer LS 50B Spectrofluorimeter. The protein concentration was determined according to Bradford [27].

4. Molecular modeling

For all synthesized molecules, the best activity was observed for compound **3b**, with a good selectivity for MAO-A (pSI = 2.70). This compound was submitted to the computational study with the aim to identify the key interaction within the catalytic site of MAO-A and MAO-B.

The first step of the computational work was the conformational analysis of the (*R*)**3b** isomer, carried out by means of 5000 steps of Monte Carlo (MC) search. Each generated structure has been energy minimized using the OPLS-AA [28a] force field and the implicit model of solvation GB/SA [28b] water as implemented in MacroModel software ver. 7.2 [28c]. With this method seven unique conformations have

Table 1
Chemical, physical and MAO inhibitory activity data of compounds **3a–y**[a] and of the reference compounds

Compound	R	R^1	Yield (%)	Mp (°C)	$pIC_{50(MAO\text{-}A)}$	$pIC_{50(MAO\text{-}B)}$	pSI[b]
3a	H	H	42	68–70	6.00	4.00	2.00
3b	H	Cl	57	108–110	6.70	4.00	2.70
3c	H	F	39	75–77	5.14	5.94	0.80
3d	H	CH_3	49	106–108	4.12	4.00	0.12
3e	H	OCH_3	35	84–86	4.71	4.00	0.71
3f	Cl	H	46	174–176	6.30	5.89	0.41
3g	Cl	Cl	36	110–111	6.70	5.00	1.70
3h	Cl	F	53	147–149	5.92	5.79	0.13
3i	Cl	CH_3	51	124–126	6.07	5.87	0.20
3j	Cl	OCH_3	45	113–115	6.00	5.00	1.00
3k	F	H	49	112–114	6.09	6.70	−0.61
3l	F	Cl	56	102–104	5.85	5.20	0.65
3m	F	F	43	104–105	6.00	6.82	0.82
3n	F	CH_3	61	108–109	5.00	6.82	−1.82
3o	F	OCH_3	54	95–97	5.92	5.00	0.92
3p	CH_3	H	56	80–82	5.25	5.35	−0.10
3q	CH_3	Cl	48	116–118	5.00	5.95	−0.95
3r	CH_3	F	43	133–135	6.12	5.79	0.33
3s	CH_3	CH_3	40	88–89	4.00	4.00	0.00
3t	CH_3	OCH_3	42	83–85	4.13	4.00	0.13
3u	OCH_3	H	32	82–83	4.20	4.60	−0.40
3v	OCH_3	Cl	35	145–146	6.08	6.07	0.01
3w	OCH_3	F	28	85–86	6.00	4.00	2.00
3x	OCH_3	CH_3	33	79–80	5.14	5.00	0.14
3y	OCH_3	OCH_3	56	76–77	5.93	5.62	0.31
MCL[c]					4.94	2.00	2.94
TOL[d]					6.42	4.82	1.60
SEL[e]					4.42	6.00	−1.58

[a] The data represent mean values of at least three separate experiments.
[b] pSI = log selectivity index = $pIC_{50(MAO\text{-}A)} - pIC_{50(MAO\text{-}B)}$.
[c] Moclobemide.
[d] Toloxatone.
[e] Selegiline.

been found within 5 kcal/mol from the global minimum energy structure. The (*S*)-isomer conformations of **3b** were obtained by mirroring the structures of the Monte Carlo structures using a module of the MOLINE method [29].

As reported in our previous work [23], the crystallographic models 2BXR [30] for the MAO-A enzyme and 1GOS [31] for the MAO-B enzyme, deposited in the Protein Data Bank (PDB) [32], were added with explicit hydrogen atoms and pre-treated with a 48 kcal/mol Å constrained energy minimization of those residues out of a radius of 15 Å from the N5 of the isoalloxazine ring, to restore the natural planarity of the isoalloxazine FAD ring and to relax the active site amino acids. The pre-treatment step was carried out with the same force field and environment reported for the MC search. After removing covalent ligands (clorgyline for 2BXR and pargyline for 1GOS), the resulting energy minimum structures were used as receptor models.

Glide software [28c] was used for docking all **3b** MC conformations with respect to the MAO-A and MAO-B models, considering a box of about 110,000 $Å^3$ centered onto the FAD N5 atom as a binding site.

In order to take into account receptor flexibility, the best 10 poses for each enantiomer in both enzymes were submitted to energy minimization. For this task, and for those following, we always applied the AMBER* force field in united atoms notation [33] coupled to the GB/SA method.

The MM–GB/SA approach [34] was used to compute the interaction energies of the optimized complexes, but no agreement was found between theoretical and experimental data. We therefore submitted the global minimum energy configurations of each complex to 1 ns of molecular dynamics (MD), at 300 K, with a time step of 1.5 fs and sampling 100 structures at regular intervals. MD configurational ensembles were used to compute the MM–GB/SA interaction energies and gave a good correlation with the experimental pIC_{50} values. Similarly a good correlation was also confirmed by applying the MM–GB/SA to the optimized ensemble obtained after full energy minimization of the MD generated configurations (OMD).

A complete list of the interaction energies is reported in Table 2.

In order to describe the different affinity of **3b** compared to the MAO isoforms at the molecular level, a graphical inspection of the MAO-A (Fig. 3a) and MAO-B (Fig. 3b) OMD global minimum energy configurations was carried out by PyMol software ver. 0.99 [35]. In both cases the (*S*)-enantiomer revealed the most favorable binding mode. MAO-A recognition showed two intermolecular hydrogen bonds, respectively, between the **3b** N2 atom and the Ser209 backbone amide and between the **3b** sp^2 propanoyl oxygen atom and the Tyr444 side-chain. The **3b** chlorophenyl ring displayed stacking contacts to the Tyr407 and to the Tyr444 side-chains and van der Waals contributions to the FAD. Stacking interactions, but less relevant, can also be addressed between the **3b** pyrazoline ring and the Phe288 benzyl ring. Such a ligand moiety also showed hydrophobic interactions with Tyr69. The **3b** propanoyl and phenyl moieties are involved in productive van der Waals contacts with Arg206 and with Leu97, Ile325, Ile335 and Leu337, respectively.

The **3b** MAO-B interaction showed a similar binding mode with respect to MAO-A, but the intermolecular contributions to the complex stabilization were quantitatively lower (Table 2). Only one hydrogen bond was observed between the **3b** sp^2 propanoyl oxygen atom and the Tyr435 side-chain. Probably the lack of such an interaction can be considered at the base of the closer ligand position with respect to the FAD. Several van der Waals contacts can be reported between the **3b** chlorophenyl ring and the cofactor. Also in the MAO-B case such a **3b** moiety was found to be involved in stacking interactions, in particular with Tyr398 and Tyr435. The **3b** phenyl ring was located in a hydrophobic cleft delimited by Leu171, Tyr326, Thr327, Leu328, Met341, Gly342, and Phe343. Particularly Phe343 was found in stacking contact. Finally, the **3b** N1 propanoyl group showed van der Waals interaction with the Tyr60 and Gln206 side-chains.

Table 2
Enantiomeric contribution, average MM–GB/SA interaction energies and differences of **3b** with respect to MAO-A and MAO-B isoforms

Ensemble	MAO-A[a]			MAO-B[a]			ΔE_{Ave}[a]
	(*R*)**3b**	(*S*)**3b**	IE_{Ave}[b]	(*R*)**3b**	(*S*)**3b**	IE_{Ave}[b]	
MD[c]	−25.97	−32.26	−29.12	−24.64	−26.90	−25.77	−3.35
OMD[d]	−29.74	−37.10	−33.42	−27.87	−29.78	−28.83	−4.60

[a] In kcal/mol.
[b] Average *R*/*S* interaction energies.
[c] MD = Molecular dynamics configurations.
[d] OMD = Optimized molecular dynamics configurations.

5. Results and discussion

The MAO inhibition data reported in Table 1 show that compounds **3a–b**, **3f–g**, **3i–k**, **3m**, **3r**, **3v** and **3w** inhibit MAO-A ($pIC_{50} = 6.00–6.92$) whereas only **3k**, **3m**, and **3n** derivatives showed good inhibitory activity against MAO-B ($pIC_{50} = 6.70–6.82$).

All compounds with halogen atom on the A and/or B rings show inhibitory activity against MAO-A and/or MAO-B. Particularly the highest MAO-A inhibitory activity was observed for compounds **3b** and **3g** ($pIC_{50} = 6.70$) substituted with chlorine on the B ring. A good activity was also observed for compound **3f** ($pIC_{50} = 6.30$) substituted with chlorine on the A ring.

Conversely compounds **3k**, **3m**, and **3n** with fluorine atom on the A ring show the highest inhibitory activity against MAO-B with $pIC_{50} = 6.70–6.82$.

The best MAO-A selectivity was measured for compound **3b** (pSI = 2.70), unsubstituted on the A ring, while the best MAO-B selectivity was observed for compound **3n** (pSI = −1.82), substituted with fluorine and methyl group on the A and B rings, respectively. When methyl and/or methoxy groups are present on the aromatic rings the compounds show poor activity against both the isoforms.

Since compound **3b** combines the best MAO-A inhibitory activity with the best A-selectivity, it was selected in the

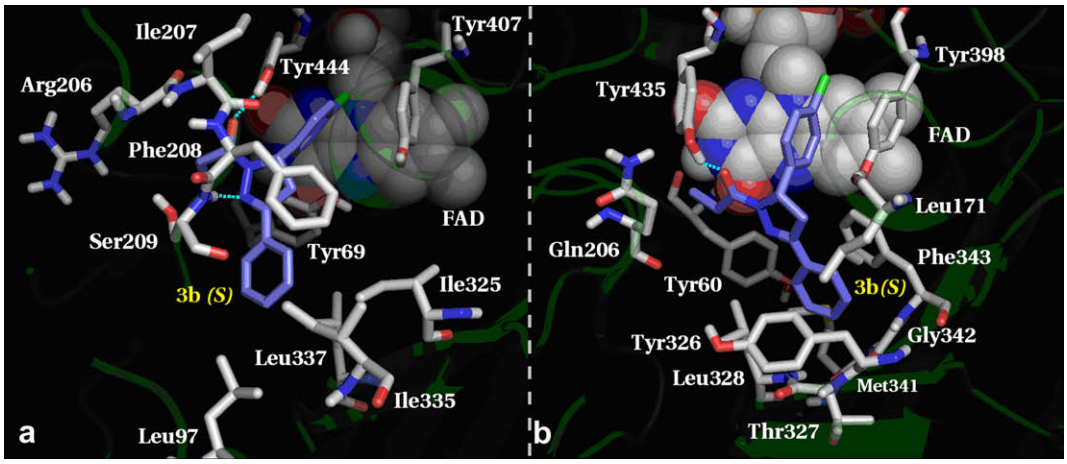

Fig. 3. MAO-A (*S*)**3b** (a) and MAO-B (*S*)**3b** (b) OMD global minimum energy configurations. Interacting residues are represented in stick and FAD cofactors are displayed as spacefill CPK rendering. (*S*)**3b** is depicted in stick with violet colored carbon atoms. Dashed cyan lines indicate hydrogen bonds (for interpretation of the references to colour in this figure legend, the reader is referred to the web version of this article).

following docking study for a better understanding of such biological properties.

In our recent experience the use of human instead of bovine models of MAO gave similar qualitative results in the docking simulations [36]. Therefore we have adopted the crystallographic model of hMAO-B available in the Protein Data Bank considering that this doesn't exactly correspond to the biological enzymes.

Compound **3b** interacted within the catalytic site of both isoforms; the complex formed with MAO-A is energetically more stable with two intermolecular hydrogen bonds. The complex formed with MAO-B showed that carbonyl of the propanoyl moiety interacted with the catalytic site by formation of a hydrogen bond with Tyr435 and the aromatic B ring was positioned in a hydrophobic pocket delimited by Leu171, Tyr32, Thr327, Leu328, Met341, Gly342 and Phe343.

Otherwise, previous docking studies on the acetyl moiety gave different results in terms of conformational distribution; the main differences were due to the acetyl oriented to the N of Lys296, located near the N5 of flavin. This binding mode was characterized by a different pattern with respect to the propanoyl reported above because the acetyl group formed a stable complex and consequently showed better activity against MAO-B.

On the basis of this research, we could show that the inhibitory activity is correlated with the presence of the halogen atoms on A and/or B rings and also with N1 substituent; in fact, the elongation of the N1 chain decreased the activity against MAO-B because of formation of an unstable complex. The results of this work will be useful in the rational design of novel selective and potent MAO inhibitors.

6. Experimental protocols

6.1. Chemistry

Melting points were determined with a Büchi capillary apparatus and are uncorrected. NMR spectra were recorded on a Brucker 400 MHz spectrometer using DMSO-d_6 or $CDCl_3$ as the solvent. Chemical shifts are reported in ppm relative to the solvent peak. Elemental analyses for C, H, and N were performed on a Perkin–Elmer 240B microanalyser, and the analytical results were within ±0.4% of the theoretical values.

Derivatives **3a–y** were synthesized as reported in literature [22].

Acknowledgements

This work is supported by a grant from MURST. We acknowledge Anton Gerada, a professional translator Fellow of the Institute of Translation and Interpreting of London and Member of AIIC (Association Internationale des Interprêtes de Conférences – Geneva) for revision of the manuscript.

Appendix. Supplementary data

Supplementary data associated with this article can be found in the online version at 10.1016/j.ejmech.2007.12.026.

References

[1] K.J. Blackburn, P.C. French, R.J. Merrills, Life Sci 6 (1967) 1653–1663.
[2] H. Takagi, T. Segawa, Serotonin, in: H. Yamasaki, H. Yoshida (Eds.), Seitaiamin (Biogenig Amines), Ishiyaku Publishers Inc., Tokyo, 1975, pp. 213–255.
[3] R. Tao, S. Hjorth, Naunyn Schmiedebergs Arch. Pharmacol. 345 (1992) 137–143.
[4] P.L. Dostert, K.F. Strolin, M. Benedetti, K.F. Tipton, Med. Res. Rev. 9 (1989) 45–89.
[5] I. Fagerval, S.B. Ross, J. Neurochem. 47 (1986) 569–576.
[6] D.E. Edmondson, A. Mattevi, C. Binda, M. Li, F. Hubalek, Curr. Med. Chem. 11 (2004) 1983–1993.
[7] J.C. Shih, K. Chen, Curr. Med. Chem. 11 (2004) 1995–2005.
[8] J.C. Shih, K. Chen, M.J. Ridd, Annu. Rev. Neurosci. 22 (1999) 197–217.
[9] W. Weyler, Y.P. Hsu, X.O. Breakefield, Pharmacol. Ther. 47 (1990) 391–417.

[10] M. Da Prada, R. Kettler, H.H. Keller, A.M. Cesura, J.G. Richards, J. Saura Marti, D. Muggli-Maniglio, P.C. Wyss, E. Kyburz, R. Imhof, J. Neural. Transm. Suppl. 29 (1990) 279–292.
[11] N.A. Garrick, D.L. Murphy, Biochem. Pharmacol. 31 (24) (1982) 4061–4066.
[12] H.Y. Yang, N.H. Neff, J. Pharmacol. Exp. Ther. 189 (3) (1974) 733–740.
[13] K.T. Demarest, D.J. Smith, A.J. Azzaro, J. Pharmacol. Exp. Ther. 215 (2) (1980) 461–468.
[14] L. Oreland, G. Engberg, Naunyn-Schmiedebergs Arch. Pharmacol. 333 (1986) 235–239.
[15] R.M. Denney, C.B. Denney, Pharmacol. Ther. 30 (3) (1985) 227–258.
[16] M.B.H. Youdim, M. Weinstock, Mech. Ageing Dev. 123 (2002) 1081–1086.
[17] B. Filip, E. Kolibas, J. Psychiatry Neurosci. 24 (1999) 234–243.
[18] H. Carageorgiou, A. Zarros, S. Tsakiris, Pharmacol. Res. 48 (2003) 245–251.
[19] E. Amaiz, V. Jelic, O. Almkvist, L.O. Wahlund, B. Winblad, S. Valind, A. Nordberg, Neuroreport 26 (2001) 851–855.
[20] W. Slikker, M.B. Youdim, G.C. Palmer, E. Hall, C. Williams, B. Trembly, Ann. N.Y. Acad. Sci. 890 (1999) 529–533.
[21] W. Maruyama, M. Weinstock, M.B.H. Youdim, M. Nagai, M. Naoi, Neurosci. Lett. 341 (2003) 233–236.
[22] F. Manna, F. Chimenti, A. Bolasco, D. Secci, B. Bizzarri, O. Befani, P. Turini, B. Mondovì, S. Alcaro, A. Tafi, Bioorg. Med. Chem. Lett. 12 (2002) 3629–3633.
[23] F. Chimenti, A. Bolasco, F. Manna, D. Secci, P. Chimenti, A. Granese, O. Befani, P. Turini, R. Cirilli, F. La Torre, S. Alcaro, F. Ortuso, T. Langer, Curr. Med. Chem. 13 (2006) 1411–1428.
[24] F. Chimenti, E. Maccioni, D. Secci, A. Bolasco, P. Chimenti, A. Granese, O. Befani, P. Turini, S. Alcaro, F. Ortuso, R. Cirilli, F. La Torre, M.C. Cardia, S. Distinto, J. Med. Chem. 48 (2005) 7113–7122.
[25] R.E. Basford, Methods Enzymol. 10 (1967) 96–101.
[26] T. Matsumoto, O. Suzuki, T. Furuta, M. Asai, Y. Kurokawa, Y. Rimura, Y. Katsumata, I. Takahashi, Clin. Biochem. 18 (1985) 126–129.
[27] M.M. Bradford, Anal. Biochem. 72 (1976) 248–254.
[28] (a) W.L. Jorgensen, D.S. Maxwell, J. Tirado-Rives, J. Am. Chem. Soc. 118 (1996) 11225–11236;
(b) W.C. Still, A. Tempczyk, R.C. Hawley, T. Hendrickson, J. Am. Chem. Soc. 112 (1990) 6127–6129;
(c) Schrodinger Inc, 101 SW Main Street, Suite 1300, Portland, OR 97204, USA.
[29] S. Alcaro, F. Gasparrini, O. Incani, S. Mecucci, D. Misiti, M. Pierini, C. Villani, J. Comput. Chem. 21 (2000) 515–530.
[30] L. De Colibus, M. Li, C. Binda, A. Lustig, D.E. Edmondson, A. Mattevi, Proc. Natl. Acad. Sci. U.S.A. 102 (2005) 12684–12689 Data deposition: www.pdb.org (PDB ID code 2BXR, 2BXS and 2BYB).
[31] C. Binda, P. Newton-Vinson, F. Hubálek, D.E. Edmondson, A. Mattevi, Nat. Struct. Biol. 9 (2002) 22–26 Data deposition: www.pdb.org (PDB ID code 1GOS).
[32] H.M. Berman, J. Westbrook, Z. Feng, G. Gilliland, T.N. Bhat, H. Weissig, I.N. Shindyalov, P.E. Bourne, Nucleic Acids Res. 28 (2000) 235–242.
[33] (a) S.J. Weiner, P.A. Kollman, D.A. Case, U.C. Singh, C. Ghio, G. Alagona, S. Profeta, P. Weiner, J. Am. Chem. Soc. 106 (1984) 765–784;
(b) D.Q. McDonald, W.C. Still, Tetrahedron Lett. 33 (1992) 7743–7746.
[34] P.D. Lyne, M.L. Lamb, J.C. Saeh, J. Med. Chem. 49 (2006) 4805–4808.
[35] DeLano Scientific, San Carlos, CA, USA.
[36] F. Chimenti, E. Maccioni, D. Secci, A. Bolasco, P. Chimenti, A. Granese, O. Befani, P. Turini, S. Alcaro, F. Ortuso, M.C. Cardia, S. Distinto, J. Med. Chem. 50 (2007) 707–712.